Applied Acoustics 74 (2013) 1463–1472

Contents lists available at SciVerse ScienceDirect

Applied Acoustics

journal homepage: www.elsevier.com/locate/apacoust

Far-field extrapolation of Maximum Noise Levels produced by individual vehicles

Teresa Bravo *, David Ibarra, Pedro Cobo

Centro de Acústica Aplicada y Evaluación No Destructiva (CAEND), Consejo Superior de Investigaciones Científicas (CSIC), Serrano 144, 28006 Madrid, Spain

ARTICLE INFO

Article history:
Received 12 November 2012
Received in revised form 10 June 2013
Accepted 14 June 2013

Keywords:
Road traffic noise
Propagation filter
Far-field extrapolation

ABSTRACT

This paper describes a combination of analytical and experimental investigations for the identification of the drivers responsible for the generation of Maximum Noise Levels (MNL) and the prediction of the extrapolated levels to the far-field positions where the receiver is situated. An on-board acquisition system composed of two microphones situated inside the engine hood and close to the right back tyre respectively provides a measurement of rolling and power-train noise. This electro-acoustic system has been shown to be able to discriminate the noisiest vehicles in different environments and for different driving behaviours. Based on this estimation of the near-field levels, we have developed a complete procedure for extrapolating the noise up to the receiver positions with a combination of analytical predictions and experimental measurements. The corrections for the extrapolated levels are due to atmospheric factors, to the spherical wave divergence term and to the absorbing conditions of the propagating surface that have been determined experimentally. For the microphone situated close to the engine we also need to characterise the acoustic properties of the engine hood. Both noise levels are extrapolated independently to the far-field position, where a comparison between prediction and measurements is performed to confirm that the methodology is reliable to estimate the remote impact of traffic noise.

1. Introduction

Attenuation of urban traffic noise has become an important challenge in highly populated cities. It constitutes one of the main sources of environmental pollution, as it has been shown that almost half of the noise in urban areas is coming from road traffic noise [1]. To reduce this nuisance, regulations for the restriction of noise emissions continue to appear to ensure a sustainable acoustic environment. However, the reduction of road traffic noise has not been proportional to the restrictions imposed [2]. Several factors can explain this trend. For instance, the reductions of individual vehicle emissions are masked by the growing tendency of the car fleet. Others reasons have been argued considering that homologation tests to estimate the maximum levels emissions are not carried out in realistic conditions [3] and they do not reproduce normal driving situations in urban courses.

A number of solutions have been proposed with different approaches to the problem. One straightforward action is to limit the number of vehicles in the traffic. However, limitation of traffic volume does not seem a realistic option for the future. Other options address several topics representing the main influence parameters on road traffic noise [3]: tyre noise, other vehicle noise components such as exhaust noise, attenuation properties of road surfaces and noise control methods such as acoustic barriers or appropriate city planning.

One part of the scientific community has claimed that the efforts made for the reduction of engine noise has been partially masked by the increase of tyre noise. As a result, tyre noise is the limiting factor for vehicle noise reduction [4]. A huge amount of specialised papers have appeared in the last two decades dealing with tyre noise, either experimental studies [5,6] or models for predicting the performance of source noise control strategies. In the last case, there are two main approaches, namely theoretical models [4,7] for the characterisation of the physical mechanisms from given properties of the road and tyres, or empirical models [8,9] estimated from correlations with experimental measurements.

In addition to previous measures, there are other considerations not directly related to noise actions on the vehicles, such as operating conditions. In particular, driving behaviour constitutes one factor that has not attracted particular attention although it has been shown that it presents a high potential for achieving noise reductions in the future [1]. Sato et al. [10] have also considered this idea analysing the extent of annoyance caused by traffic noise in different building at varying distances from the road traffic and for a varying number of vehicles. They have considered the number

* Corresponding author. Tel.: +34 91 5618806; fax: +34 91 4117856.
E-mail address: teresa.bravo@caend.upm-csic.es (T. Bravo).

0003-682X/$ - see front matter © 2013 Elsevier Ltd. All rights reserved.
http://dx.doi.org/10.1016/j.apacoust.2013.06.006

of events and the noise levels as two independent variables, and have found that the number of noise events did not influence the extent of annoyance. They have outlined also that there was a strong correlation between annoyance and Maximum Noise Levels, and concluded that actions to control road traffic noise should be directed on noisy vehicles rather than on the limitations of the traffic flow.

Actions focused on noisy drivers have been oriented mainly towards awareness programs about noise and its effects, but supplementary efforts are needed for dealing with the problem more practically. This work presents a complete framework for the acquisition, analysis and extrapolation of urban transportation noise focusing on the driving behaviour. A system is described for the acquisition of the sound pressure levels generated from individual vehicles. This on-board acquisition system has been tested using several diesel and petrol engines along urban and suburban courses, and has been shown to be able to identify the drivers causing the highest noise levels and their discrimination. It could be used, for example, for regular vehicles testing or at specific control points placed in problematic areas as "noise-enforcement radars" for the vehicles circulating nearby. The results from the embarked acquisition system are summarised in Section 2 of the paper: they provide an estimate of the near-field levels recorded in real time. It is then necessary to propagate these near-field pressure data to the receiver positions over a combination of ground surfaces composed of different materials. Special attention has been paid to the proper identification of the impedances of the ground surfaces: the two-microphones method has been used for the characterisation of the ground physical parameters, which are then considered in the extrapolation model. This model has been developed using a combination of analytical formulation and experimental measurements. The complete procedure is explained in detail in Section 3. Finally, the analytical predictions are validated against a set of experimental pass-by measurements that confirm the suitability of the methodology (Section 4). The paper concludes with a summary of the main results obtained and directions for future work.

2. Near-field measurement system

To distinguish noisy drivers from the total traffic fleet, an electronic acquisition system installed on the vehicle has been designed [11]. The number and positions of sensors to capture the relevant information should be determined. For the sake of simplicity and considering the work done in previous European projects [12,13], one microphone has been situated in the proximity of the engine to acquire the power-train noise, and a second microphone is positioned close to the tyre for the rolling noise acquisition. It has been shown that power-train noise dominates at low driving speeds, around 40–50 km/h for light vehicles, and 50–60 km/h for heavy vehicles. When increasing the velocity, tyre noise becomes dominant, although at very high speeds it is the aerodynamic noise which produces the major part of the vehicle noise [12,13].

The measurements have been performed using two microphones Shure MX183 calibrated with a B&K 4231 sound source. They are glued to the vehicle with a mastic adhesive at the positions shown in Fig. 1. The microphone preamplifiers were modified to increase the dynamic range up to 129 dB. As it can be appreciated, the rolling noise microphone has been protected against aerodynamic noise with a nose cone that modifies its frequency response function introducing a low pass filter with a cut-off frequency at 5 kHz [11]. However, it does not significantly affect the acquired signals as the tyre noise spectrum quickly decreases above 1 kHz [14].

A near-field characterisation of the noise radiated by each individual vehicle has been performed with two vehicles in the segment B [12], a Seat Ibiza with either petrol or diesel engines. An example of these measurements for both the urban and suburban courses is presented in Fig. 2, that confirms the trends already observed for engine and tyre traffic noise [14]. Each vehicle has been driven by five persons (three men and two women) through one urban and one suburban driving course. At the same time, the information concerning the driving behaviour is acquired using the vehicle CAN BUS interface. The engine speed, the engine load and the accelerator positions were also recorded. From the group of five persons, one was required to drive in a more sportive way. A complete description of the instrumentation, driving conditions, scenarios and results appears in Ibarra et al. [11], and it will not be described in detail here. To summarise the main conclusions, we will indicate that, considering both the global equivalent level and the level histogram, the on-board system is able to discriminate noisy drivers from the mean traffic stream. Engine noise results arising from this driving behaviour were between 5 and 9 dB higher, in average, than those produced from the rest of the drivers. The same trend was observed for the rolling noise, providing noise levels on average between 3 and 5 dB in excess with respect to the other four drivers.

3. Far-field extrapolation

The objective of this section is to develop an analytical model for the propagation of each individual vehicle noise source to the far-field positions accounting for the ground effects due to the acoustical properties of the propagation path. The procedure described in Section 2 for the acquisition of the levels produced by noisy drivers and their identification provides us with a set of near-field data for each vehicle, composed of engine and tyre microphone signals. Based on these measurements, we present here a complete procedure for the levels extrapolation in terms

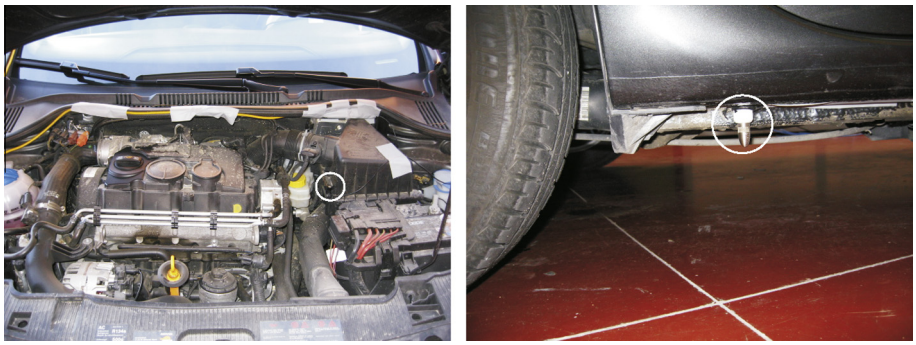

Fig. 1. The position of the microphones close to the engine (left) and close to the tyre (right).

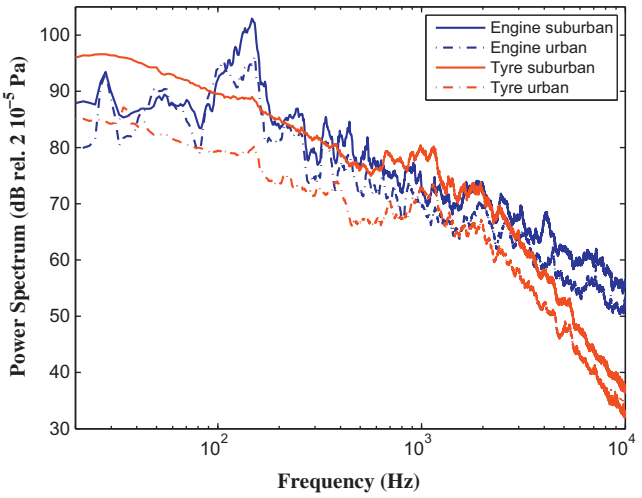

Fig. 2. Power spectrum of the signal provided by the microphone situated close to the engine (blue) and close to the tyre (red) for the suburban (solid) and urban (dashed-dotted) courses for the diesel Seat Ibiza. (For interpretation of the references to colour in this figure legend, the reader is referred to the web version of this article.)

of the receiver position, the atmospheric conditions and the proportion of porous materials and soft ground presented in the semi-infinite road-side surfaces. The extrapolation of the two noise sources will be treated separately in the following subsections.

3.1. Rolling noise extrapolation

The signals acquired by the microphone situated close to the tyre should be propagated to the positions where the receiver is situated. We then need an estimation of the transfer function between the source and the receiver position, also called the propagation filter, defined as the level difference between the near-field measurements, L_{nf}, and the far-field levels, L_{ff}. In this work we have developed an analytical model inspired by the work presented by Anfosso-Lédée et al. [15] and Cho and Mun [16]. The near field levels are assumed to be generated by four point sources located at the tyre-road contact positions, as indicated in Fig. 3. For each tyre, they depend on the sound power level of the individual source, on the geometrical divergence term and on attenuation values, that comprise the absorption of the acoustic energy by the air and the effects due to the influence of the environment on the propagation (ground absorption, horn effect, etc.). For each tyre, the near-field levels read

$$L_{nf,t} = L_{Wt} + 10\log_{10}\left(\frac{1}{4\pi r_{nf,t}^2}\right) + Att_{nf,t}, \tag{1}$$

where L_{Wt} is the sound power level due to one tyre, $r_{nf,t}$ the distance from one tyre to the near-field microphone, and $Att_{nf,t}$ the attenuation level in the path from the tyre monopole source to the rolling noise microphone. These quantities are all the same for the four tyres. The propagated levels at the receiver position correspond to the incoherent sum of the near-field power levels. Considering the symmetry of the problem (Fig. 3) we can see that the levels due to the first and second tyre are the same than those due to the third and fourth tyre, respectively. The far-field levels due to the rolling noise can then be expressed as

$$L_{ff,t} = 10\log_{10}\left(2\cdot 10^{\frac{L_{t1}}{10}} + 2\cdot 10^{\frac{L_{t2}}{10}}\right), \tag{2}$$

where L_{ti} is the sound pressure level due to one tyre ith at the far-field position. It takes the expression

$$L_{ti} = L_{Wt} + 10\log_{10}\left(\frac{1}{4\pi r_{t,i}^2}\right) + Att_{t,i}, \tag{3}$$

where i can vary between 1 and 4, $r_{t,i}$ is the distance from the tyre ith to the far-field microphone, and $Att_{t,i}$ the attenuation level in the path from the monopole source i to the far-field position. Particularising Eq. (3) for the first and the second tyre, and substituting the expressions into Eq. (2), we obtain

$$L_{ff,t} = L_{Wt} + 10\log_{10}\left(\frac{1}{4\pi r_{t1}^2}\right) + Att_{t1} + 10\log_{10}\left[1 + \left(\frac{r_{t1}^2}{r_{t2}^2}\right)10^{\frac{Att_{t2}-Att_{t1}}{10}}\right] + 10\log_{10}(2). \tag{4}$$

The transfer function, defined as the level difference between near and far-field levels, can be calculated from Eqs. (1) and (4), and takes the expression

$$H_{nf,ff,t} = 10\log_{10}\left(\frac{r_{t1}^2}{r_{nf,t}^2}\right) + Att_{nf,t} - Att_{t1} - 10\log_{10}\left[1 + \left(\frac{r_{t1}^2}{r_{t2}^2}\right)10^{\frac{Att_{t2}-Att_{t1}}{10}}\right] - 10\log_{10}(2), \tag{5}$$

which is similar to Eq. (8) from Ref. [15] deduced considering that the four tyres are substituted by one equivalent source situated at the centre of the vehicle, and evaluated at the (Close ProXimity) and CPB (Controlled Pass-By) positions [17,18]. It should be outlined here that we do not intend to apply the measurement positions described in the standards for determining the contribution of the road surfaces to the propagated levels, as the aim is to develop an on-board acquisition system able to perform online noise measurements to be analysed and controlled later on. The transducer positions are then selected based on the most convenient choice for real-time operation.

For the calculation of the transfer function between the source and the receiver (Eq. (5)), we need expressions for the attenuation

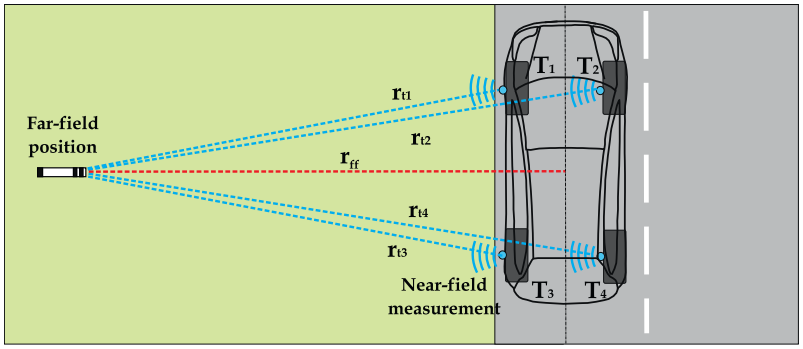

Fig. 3. Physical configuration for extrapolation of the rolling noise from near-field measurements to far-field levels.

values from the two tyres to the receiver position, and the attenuation values from one tyre to the near-field microphone. Factors to be considered include the atmospheric conditions, that influence the sound speed, the air density and viscosity, and the acoustic impedance of the ground. The air absorption as sound propagates through the atmosphere has to be calculated also, which depends on frequency and relative humidity. For these considerations we need to determine the atmospheric variables when performing the measurements and apply the American Standard ANSI S1.6 [19]. However, for the frequency range and the physical configuration of the problem, the influence of these factors on the results is small in comparison with the effect of the ground surfaces, considered in the next section.

3.2. Determination of the ground impedance

A simple analytical model exists when analysing the propagation of sound in a homogeneous medium and due to a point source located above a semi-infinite locally reacting porous ground. The model is based on ray theory, considering that the resulting sound field at any point will be the contribution from the direct path coming from the sound source, and the reflected path, influenced by the acoustic properties of the propagating surface. The attenuation of the reflected sound will depend on the frequency, and will be more important towards increasing angles. The typical problem geometry is represented in Fig. 4. The source is situated at a height h_s and radiates over a flat soft ground. The sound pressure received at the far-field positions, situated also above the ground, will then be expressed as the two-term expression [20,21]

$$\phi = \frac{e^{ikR_1}}{4\pi R_1} + Q_1 \frac{e^{ikR_2}}{4\pi R_2}. \tag{6}$$

In this equation, the distances R_1 and R_2 are linked to the direct and reflected rays from the source to the receiver, respectively. The reflected path will be influenced by the properties of the semi-infinite surface. The reflection coefficient of the spherical wave, Q_1, accounts for these considerations. A mathematical description has been presented, for example in [20,21], that depends on R_2, on the incidence angle and on the surface acoustical properties, defined by the specific normalised admittance, $\beta = 1/Z$. Due to its simplicity, we have selected the Delany and Bazley [22] model that provides an analytical description of the material absorption properties considering only one parameter, the flow resistivity σ. The complex propagation constant and the normalised impedance of the porous ground are then given by a semi-empirical model that takes the expressions [21]

$$k = \left(\frac{\omega}{c_0}\right)\left[1 + 0.0978\left(\frac{\rho_0 f}{\sigma}\right)^{-0.700} + i \cdot 0.189\left(\frac{\rho_0 f}{\sigma}\right)^{-0.595}\right], \tag{7}$$

$$Z = Z_0\left[1 + 0.0571\left(\frac{\rho_0 f}{\sigma}\right)^{-0.754} + i \cdot 0.087\left(\frac{\rho_0 f}{\sigma}\right)^{-0.732}\right], \tag{8}$$

with c_0 and ρ_0 being respectively the velocity and density of air, f the frequency and ω the angular frequency.

Data for the flow resistivity can be obtained from the specialised literature. For instance, in the European Harmonoise project [12], values for Dense Asphalt Concrete surfaces (DAC) and for Stone Mastic Asphalt surfaces (SMA) with different chipping sizes can be found. Examples of the transfer functions between the rolling microphone and the receiver position have been presented previously by the authors [23] using the one-parameter model for a DAC 0/19, the ISO road surface according to ISO 10844, and the Hamet et al. [20] model for a porous asphalt material. However, to obtain a better agreement between experimental measurement and model prediction, it has been decided to characterise experimentally the particular surface used for the measurement. We have followed recommendations of the American Standard ANSI S1.18 [24], generating a sound pressure field with a source situated at 0.5 m height above the ground, and two identical microphones situated at a height of 0.88 and 0.08 m respectively (Fig. 4). The horizontal separation distance between source and microphones has been fixed to 3 m. This configuration has been shown to minimise the measurement errors in the frequency range between 250 Hz and 4 kHz for outdoor sound propagation prediction [25]. The point source was approximated by a spherical loudspeaker of 20 cm diameter, and the two free-field microphones B&K 4191-L were protected with windscreens, as it can be appreciated in Fig. 4. The loudspeaker was driven by a pseudo-random signal generated by a home-made virtual instrument created in Matlab for the determination of the impulse response functions between input and measured signals. To avoid the influence of undesired reflexion and background noise, the impulse response signals were windowed and converted to the frequency domain. Each measurement has been repeated and averaged over four different relative positions over the surface of analyses. During the measurements, the temperature was 12 °C, the relative humidity had a value of 48%, the atmospheric pressure was 924 mb and the wind speed was varying between 1.2 m/s and less than 3 m/s in all cases.

For determining the surface flow resistivity we have calculated the level difference between top and bottom microphones for each frequency,

$$\Delta L(\mathrm{dB}) = L_{top} - L_{bottom} = 20\log_{10}\left|\frac{p_{top}}{p_{bottom}}\right|. \tag{9}$$

We can compare these experimental values with those calculated by the analytical prediction assuming that the surface can be described by the one-parameter model, Eqs. (7) and (8), that provides an estimate of the real and imaginary parts of the acoustic impedance as a function of the physical parameters. An optimisation procedure has then to be carried out using the mean-square

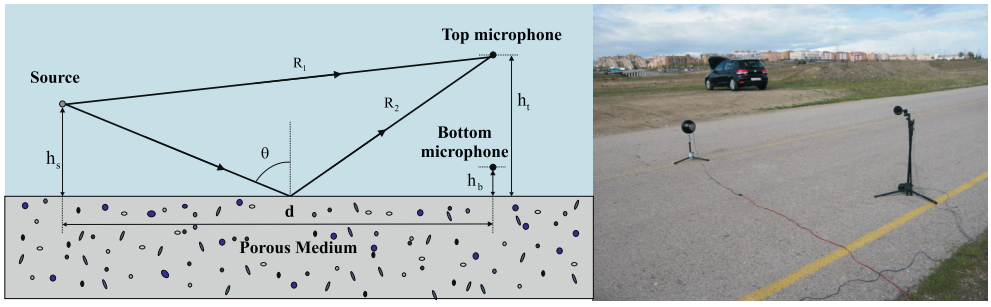

Fig. 4. Two-microphone configuration method for determination of the ground impedance and measurement of the level difference for the porous asphalt.

error between the analytical and the measured values. The optimal flow resistivity is found when the residual norm is minimal. Using this procedure, we have performed the experimental characterisation of the level differences in the frequency range (250, 4000) Hz, for a porous asphalt and found an optimal value for the asphalt flow resistivity equal to $\sigma = 8000$ kPa s m^{-2}. We can then calculate analytically the terms $Att_{t,1}$ and $Att_{t,2}$ assuming a homogeneous porous asphalt between the rolling sources and the receiver. However, as indicated in Fig. 3, there exists a discontinuity of impedance in the propagation path. It has thus been included in the study. A solution for the combination of surfaces composed of porous asphalts and grass-land has been considered by Rasmussen [26], that shows that it can be obtained assuming an infinite line array of virtual sources situated at the impedance discontinuity position. It is then also necessary to characterise the natural soil presented at the receiver positions, carried out in the same way as for the asphalt. We have measured the averaged ΔL for the grass-land and calculated the optimal impedance values minimising the mean-square error between model and measurements, obtaining a value of $\sigma = 500$ kPa s m^{-2}. The measured values and those calculated with the optimal flow resistivity are presented in Fig. 5 for the two different grounds, the asphalt (left) and the grass-land (right).

Finally, we still need to provide expressions for the term $Att_{nf,t}$ of Eq. (5), that corresponds to the attenuation levels in the path from the tyre source to the corresponding near-field microphone. We cannot apply the same methodology already used for the propagation to the far-field positions, due to the multiple reflections in the proximity of the vehicle. These considerations could be taken into account with numerical methods, but in this work we intend to analyse the limitations of using a combination of empirical and analytical techniques for road noise propagation. Previously [23], we have included these factors using directivity functions inspired by the work presented in the European project Harmonoise [12], that provides analytical expressions for both noise sources and both horizontal and vertical directivity as a function of the vehicle category and vehicle speed. In this work we have completed these corrections in view of the experimental data acquired by the embarked rolling noise microphone. This point will be discussed in Section 4.

3.3. Power-train noise extrapolation

The levels due to the power-train noise have also a contribution in the far-field. This noise source has to be extrapolated independently, and added incoherently with the tyre-induced noise at the receiver position. Extrapolation of rolling noise has been widely studied and analytical formulations are available when considering a simplified physical system, as explained in the precedent

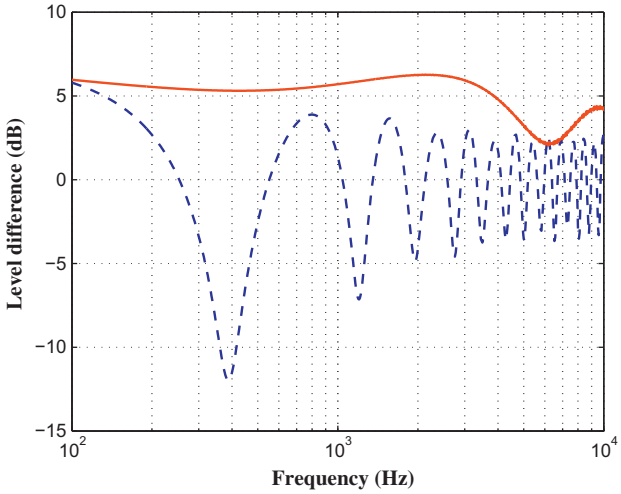

Fig. 6. The level difference between the receiver position and the power-train source (dashed) and rolling source (solid) when considering a mixed grass-land and porous asphalt propagation surface.

sections. On the other hand, there is not a straightforward expression for the extrapolation of the noise levels acquired by the microphone situated inside the engine hood. A new set of analytical expression is presented in this section. Following the method of Section 2.1, we should express the sound pressure levels acquired at the near-field and far-field microphones, and calculate the transfer functions as the level difference between both expressions.

The sound pressure acquired by the microphone in the proximity of the engine, due to the vehicle power-train (pt), valid in the direct field close to the engine source, is given by

$$L_{nf,pt} = L_{Wpt} + 10\log_{10}\left(\frac{1}{4\pi r_{nf,pt}^2}\right) + Att_{nf,pt}, \tag{10}$$

where L_{Wpt} is the sound power level due to the power-train source, $r_{nf,pt}$ the distance from this source to the microphone inside the engine hood and $Att_{nf,pt}$ the attenuation level in the path from the source to the engine microphone. We now assume one noise source situated outside and at the centre of the engine hood that is creating a sound pressure level at the far-field position expressed by

$$L_{ff,pt} = L_{Wpt,out} + 10\log_{10}\left(\frac{1}{4\pi r_{ff,pt}^2}\right) + Att_{ff,pt}, \tag{11}$$

where $L_{Wpt,out}$ is the sound power level due to the source situated outside the engine hood, $r_{ff,pt}$ the distance from the external source to the far-field position, and $Att_{ff,pt}$ the attenuation level in the path

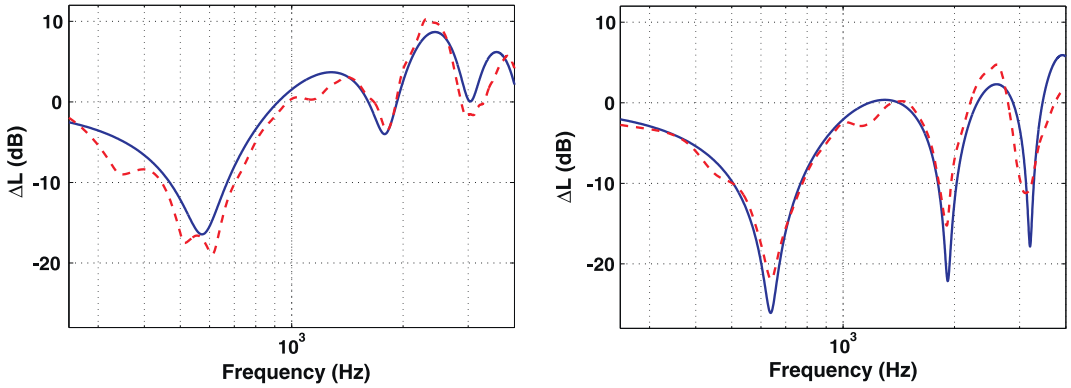

Fig. 5. The level difference for the porous asphalt (left) and the grass-land (right) determined experimentally (dashed) and calculated with the Delany and Bazley model (solid) for the optimal values of the flow resistivity.

from the external source to the receiver. The transfer function from the power-train source to the receiver is defined as the level difference between near and far-field levels, that can be calculated from Eqs. (10) and (11),

$$H_{pt} = (L_{Wpt} - L_{Wpt,out}) - Att_{ff,pt} + 20\log_{10}\left(\frac{r_{ff,pt}}{r_{nf,pt}}\right). \quad (12)$$

To obtain this expression, it has been assumed that the term $Att_{nf,pt}$, the attenuation inside the engine hood in the path from the source to the internal microphone, is negligible in comparison with the other attenuation terms. The first term, the level difference between incident and radiated power, is the Transmission Loss of the engine hood, $TL = L_{Wpt} - L_{Wpt,out}$, that will be determined in the next section. The attenuation values from the source to the far-field positions, $Att_{ff,pt}$, can be calculated as indicated in the previous section for the rolling noise. An example of the values that could be obtained is presented in Fig. 6, superimposed to the values of the propagation filter for the rolling source, $Att_{t,2}$ (Eq. (5)). We have considered the real situation with a layer of porous asphalt 2.4 m long from the vehicle axis, and a grass-land soil at the receiver position, using the corresponding optimal flow resistivities. The total distance between the vehicle and the receiver has been taken as 7.5 m, as recommended by the European Standard ISO 11819 [17], with a height of 1.2 m. As it can be appreciated, interaction between the direct and reflected sound fields is more uniform for the rolling source, assumed to be 0.04 m high, than for the engine source, situated at 1.1 m above the ground.

3.4. Engine hood Transmission Loss

The extrapolation of the power-train noise using Eq. (12) requires the determination of the insolating properties of the vehicle engine hood, that has been considered as an acoustic partition coupled to a small enclosure where the engine is situated.

To characterise the incident and radiated sound power, a spherical source has been situated inside the engine hood, as it can be seen in Fig. 7 (hood opened), driven by a pseudo-random signal. The incident sound power has been calculated using a microphone FONESTAR FOX 2214 situated inside the cavity (Fig. 7). The measured impulse response has been converted to the frequency domain, and the incident power is related to the mean-square sound pressure in the proximity of the engine, $\langle p^2_{source}\rangle$, by [27] as

$$\Pi_{Inc.} = \frac{\langle p^2_{source}\rangle S_h}{4\rho_0 c_0}, \quad (13)$$

where S_h is the surface of the hood.

For the estimation of the radiated sound power, we have used a set of microphones uniformly distributed on a semi-circle surrounding the vehicle, with a radius of 1.2 m, as indicated in Fig. 7. The separation angle between the microphones has been fixed to 5°. To cover the whole semi-circle, it has been necessary to take 37 measurement points. The transmitted sound power is obtained considering that we have a monopole source radiating in free field, and it is calculated as [27]

$$\Pi_{trans} = \frac{\langle p^2_{out}\rangle S_{rad}}{2\rho_0 c_0}, \quad (14)$$

where $\langle p^2_{out}\rangle$ is the mean-square sound pressure outside the vehicle and S_{rad} the observation surface. The Transmission Loss (in dB) may thus be evaluated from [27]

$$TL(\omega) = 10\log_{10}\left(\frac{\Pi_{Inc.}(\omega)}{\Pi_{trans}(\omega)}\right) \quad (\text{dB}). \quad (15)$$

An example of the results that can be obtained with this procedure is presented in Fig. 8, that shows a similar behaviour to the TL values obtained for a thin steel panel partition.

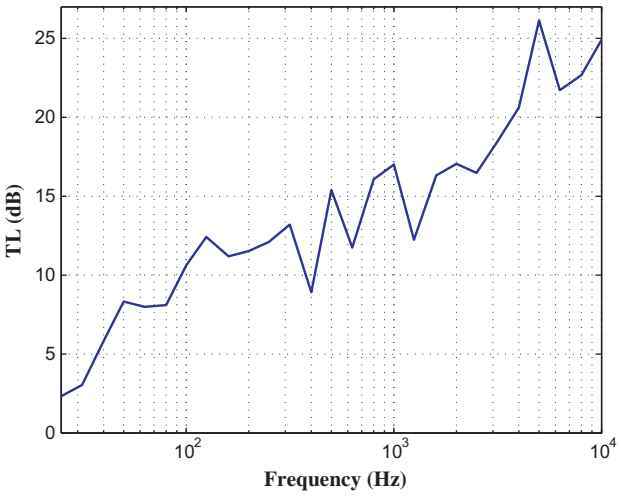

Fig. 8. Measured Transmission Loss for the vehicle engine hood.

4. Experimental comparison

To validate the proposed extrapolation model, a set of experimental measurement has to be acquired simultaneously at the near-field and far-field positions. The starting point to perform the comparison are the signals acquired by the on-board acquisition system, used as inputs to the analytical propagation filter for each source independently, that are added at the receiver position. The propagated results should then be compared with the

Fig. 7. Position of the spherical source and microphone inside the engine hood (left), and the external hemispherical distribution of microphones (right) for the determination of the engine hood Transmission Loss.

Fig. 9. The body-pack transmitter for the embarked wireless system of the rolling microphone (left) and the far-field microphone for measuring the pass-by noise (right).

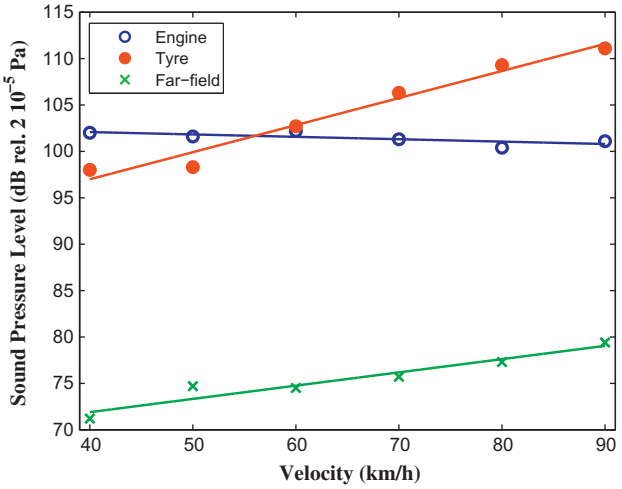

Fig. 10. Measured sound pressure levels as a function of the velocity for the microphone close to the engine (empty circles), close to the tyre (solid circles) and in the far-field (crosses).

corresponding experimental far-field measurements. The details are discussed in the next subsections.

4.1. Near-field and far-field measurements

The near-field measurements recorded by the on-board acquisition system have been carried out over a straight route in an area isolated from traffic and with low background noise. A light vehicle in the B segment was driven by the same person for a set of six different vehicle speeds from 40 to 90 km/h, namely in 2nd gear when the vehicle was circulating at 40 and 50 km/h, in 3rd gear at 60 and 70 km/h and in 4th gear at 80 and 90 km/h. For each pass-by velocity, the driver was taking a fraction of the course to reach the selected speed, that was then maintained constant over a straight portion of the road of about 500 m length. Initial measurements were made using two different acquisition systems, one embarked on the vehicle to record the near-field signals, and a second one in charge of the far-field measurements towards the receiver position. This set-up, however, shows some synchronisation problems that can be avoided using wireless embarked systems. Hence, three Sennheiser wireless systems with body pack transmitter were used for each of the near-field microphones shown in Fig. 1. This system can be seen in Fig. 9 (left) for the rolling noise microphone.

Measurements of the far-field and near-field levels were performed synchronously. As it can be seen in Fig. 9 (right), a Fonestar FXX 2214 microphone was situated at 7.5 m from the vehicle axis, at a height of 1.2 m, and protected by a wind screen. The near-field microphones have been both covered by a nose cone to reduce contamination by the aerodynamical noise. The sensitivities of the three sensors have been characterised with a B&K 4231 calibrator. The signals have been analysed with the system PULSE Labshop Version 14.0.1 from B&K. The measurements have been carried out with overcast sky and with low wind speeds, to minimise turbulence due to thermal and wind gradients. The atmospheric conditions were a temperature of 12.6 °C, a relative humidity of 58%, an atmospheric pressure of 924 mb and a wind speed varying between 3 and 5 m/s. The levels captured by the three microphones as a function of the engine velocity are presented in Fig. 10. Near-field measurements are presented as circles and far-field levels are shown as crosses. As expected, power-train levels are predominant for low vehicle speeds whereas the trend is inverted when increasing the velocity beyond 60 km/h. The curves obtained by linear regression with the six experimental measurements are also superimposed. Most of the points fit well within the corresponding lines, except the results at 50 km/h. When analysing in detail the temporal signals at 50 km/h, a problem was detected on the total length of the acquired measurements that do not provide the correct levels. This signal has thus been removed from the subsequent analysis.

4.2. Comparison with the analytical model

The near-field signals for each pass-by velocity have been introduced in the analytical model and extrapolated to the receiver position. They have been compared with the experimental far-field levels acquired by the microphone situated at 7.5 m from the vehicle. We then need to provide an expression for the factor $Att_{nf,t}$, that appears in Eq. (5) and accounts for the attenuation between the tyre source and the rolling noise microphone situated nearby (Fig. 1). In previous works [23], the authors have implemented the directivities obtained in the Harmonoise EC project [12], that provides analytical expressions for both lower and upper sources, to include corrections due to diffraction by the vehicle body shape. Examples of the directivities and the results obtained can be found in Ref. [23]. It has been shown that when considering the medium and high frequency range (500 Hz–10 kHz), the agreement between experimental and predicted extrapolated levels is good, with differences that are below 1 dB in the global levels for all pass-by velocities. However, the agreement degrades towards the low frequency range, typically below 500 Hz. We made the hypothesis that these differences could be due to aerodynamic noise contaminating the rolling noise microphone signal. Several authors [28,29] have performed experimental measurements to evaluate the effect of the disturbing noise generated when the on-board acquisition system moves with the vehicle in the air. They have presented results relating the noise levels due to aerodynamic effects as a function of the vehicle speed, testing several microphone windshields. The measurements were first performed in a laboratory with a wind turbine producing several speed flows,

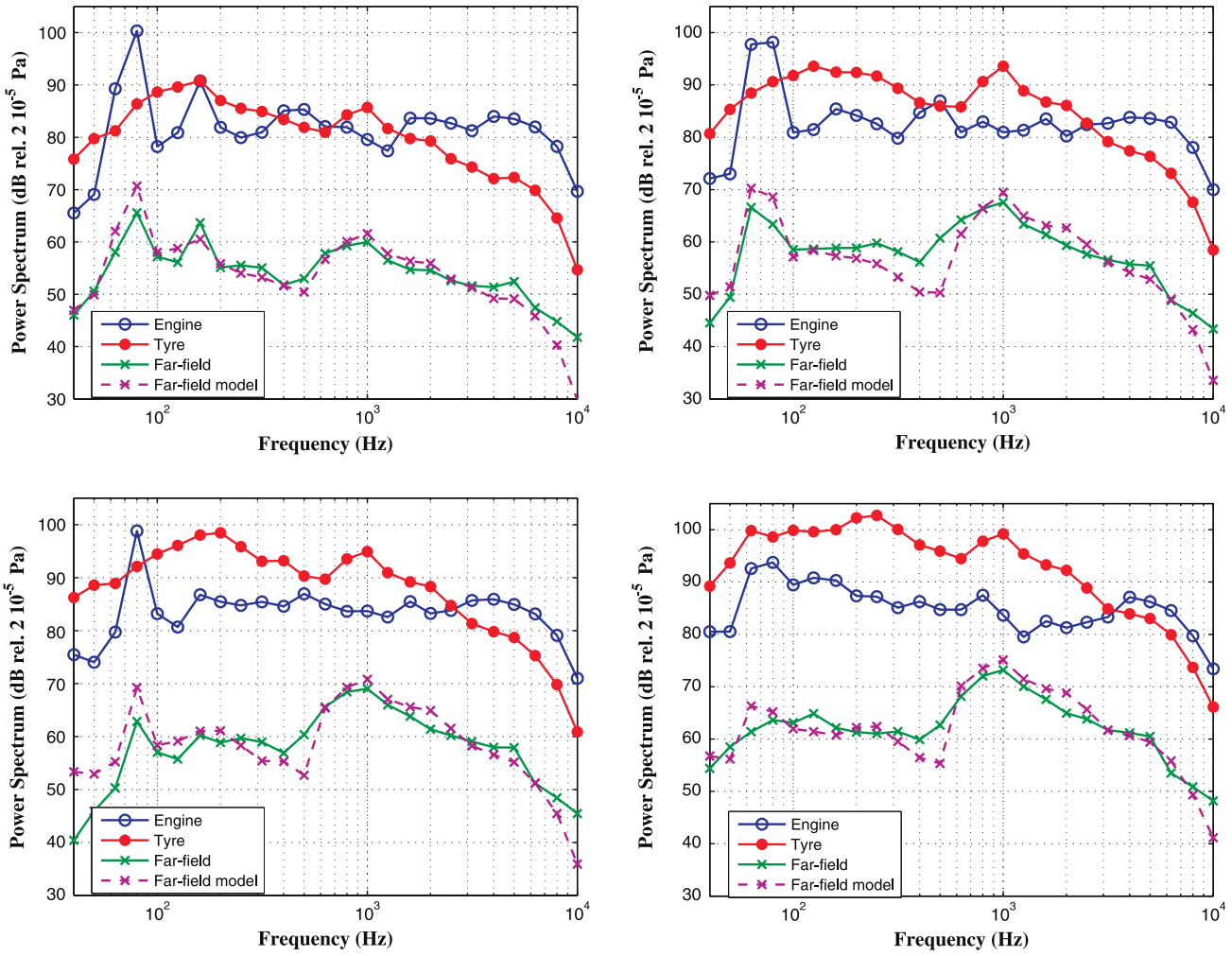

Fig. 11. Power spectrum of the experimental noise levels measured by the engine microphone (empty circles), by the rolling microphone (solid circles), at the far-field microphone (crosses) and calculated with the analytical model (dashed crosses) for pass-by velocity of 40 km/h (top left), 60 km/h (top right), 70 km/h (bottom left) and 90 km/h (bottom right).

Table 1
Overall levels (dB) measured in the near-field (engine and rolling) and far-field (ff, measured), predicted with the analytical model (ff, predicted) and difference between both of them.

Vel (km/h)	Gear	L_{engine}	$L_{rolling}$	$L_{ff,measured}$	$L_{ff,predicted}$	ΔL
40	2ª	102.0	97.9	71.2	73.4	2.2
60	3ª	102.1	102.7	75.0	76.5	1.5
70	3ª	101.3	106.3	75.8	77.3	1.5
80	4ª	100.4	109.3	77.4	79.0	1.6
90	4ª	101.1	111.1	79.4	80.8	1.4

and outdoors in real driving conditions, quantifying the wind speed around the microphone position using Pitot tube sensors. They presented noise levels in third-octave bands from 12.5 Hz to 20 kHz, for vehicle speeds starting in 50 km/h, up to 130 km/h [28]. They stated that aerodynamic noise is very important in the low frequency range, with levels above 90 dB for a 50 km/h speed, and going beyond the 110 dB for 130 km/h. They concluded that in the low frequency range this noise influenced significantly the levels acquired by the microphone and recommended the use of a filter to decrease the aerodynamic noise pollution. Other option was to consider the frequency range between 315 Hz and 5 kHz, denoted as "CPX frequency zone" for the compositions of the global sound levels.

In addition to the previous considerations, it should also be outlined that when considering CPX measurements [18], the recording microphone is mounted on a designed trailer at a distance of 0.28 m out of the tyre plane, with the purpose of minimising the noise coming from the power train, auxiliary systems, air turbulence and sound reflections from the vehicle body. This is not the case in our situation as the recording microphone positions have to comply with practical and sustainable conditions for the on-board acquisition of the near-field levels. As explained in Section 2, the placement of the sensor is selected in the plane of the tyre considering the feasibility for real-time operating conditions. We should consider then that the tyre/road emission is not omnidirectional as it is generally assumed in noise calculation, with directivity patterns with highest values appearing in the front of the tyre [30], where the rolling noise microphone is situated.

A near-field filter has to be designed to remove all these noise contributions before the far-field extrapolation. For the sake of simplicity and to maintain an analytical formulation for the extrapolation filter, we have decided to use a filter following the mathematical form proposed in the Harmonoise project for the near-field levels, adjusting the coefficients according to our experimental data. The proposed filter takes then the expression

$$\Delta L_{horn} = L_{nf,t} - K \cdot 10\log_{10}\left(\frac{V}{V_{ref}}\right). \quad (16)$$

ΔL_{horn} are the resulting levels after the near-field filter application, K is a constant that has to be adjusted to the set of experimental data, V is the pass-by velocity and V_{ref} is the reference velocity, that has been taken as 30 km/h. In the Harmonoise project, the coefficients are frequency dependent. In this work, we have selected a constant value of 0.3 for the frequency bands up to 800 Hz, and zero elsewhere. Although the accuracy of this near-field filter could be much more improved, it has been selected as a trade-off between simplicity and satisfactory agreement with the experimental extrapolated results. A comparison between the extrapolated values resulting from the analytical model and those measured at the receiver position are presented in Fig. 11, for pass-by velocities of 40, 60, 70 and 90 km/h. The near-field values measured with the acquisition system are also presented to illustrate their contribution to the far-field attenuated values for each centre frequency band. It can be seen that the agreement between both curves, considering the wide range of frequencies analysed (from 20 Hz to 10 kHz), is reasonably good. Although the differences are a bit more pronounced in the central frequency band of 500 Hz, they could be improved by adjusting the filter coefficient with frequency. To do that, we will need to perform a statistical treatment of the problem, with a higher number of experimental data. Differences can also be appreciated in the high frequency bands analysed, that may be due to the flow resistivity value used for the asphalt and the grass, optimised for a best fit up to 4 kHz.

To further analyse the differences between prediction and experiment, we have summarised in Table 1 the results obtained for all the pass-by velocities considered, presenting the near-field overall values, and the corresponding far-field overall levels. The difference between measured and analytical results is shown in the last column.

As it can be seen, the agreement between experimental and predicted levels is satisfactory for all the pass-by velocities, with differences lower than 2.2 dB for all the pass-by velocities. We conclude that, despite its simplicity, the developed semi-analytical formulation provides a correct estimation of the far-field extrapolated levels, that could then be compared in confidence with the current normative for road noise emissions in order to take control actions on the individual drivers if required.

5. Summary and conclusions

Although a huge amount of efforts has been made for the reduction of road traffic noise concerning design of low noise tyres and "quiet" materials for vehicle components and road surfaces, complementary solutions for the reduction of tyre noise are still demanded, so that their combined effects contribute to achieve optimal noise attenuation results. In particular, the driving behaviour and its control may have an important impact in reducing traffic noise.

The objective of this work is to develop an analytical model to predict the levels of sound that propagates from the vicinity of vehicles to the position of the receiver, situated in the far field. A set of theoretical and experimental works has been carried out for the design of an electroacoustic system embarked on a vehicle, for the acquisition of near-field measurements and the discrimination of the particular drivers responsible of the MNL. It is composed of two microphones recording rolling noise and power-train noise, and acquires also information concerning the driving behaviour. This system has been tested using several diesel and petrol vehicle engines along urban and suburban courses with five different drivers.

Application of control actions on these drivers requires, however, the extrapolation of the levels acquired in the near-field to the receiver position in the far-field. At this point, the estimated far-field noise emissions should comply with the corresponding normative, and if the radiated sound levels exceed those allowed, actions on these drivers could be taken. We have developed an extrapolation filter for both near-field microphone signals combining an analytical formulation and measurements, avoiding the use of numerical techniques. The attenuation between the near-field and far-field positions is mainly affected by the acoustical properties of the ground surface, modelled using the Delany and Bazley law, and that requires only knowledge of the material flow resistivity. As the propagation surface is not uniform, but presents a discontinuity of impedance due to different soils between the source and the receiver positions, we have paid particular attention to the acoustical propagation over a hybrid surface composed of porous asphalt and grass-land. The determination of the flow resistivity for both materials has been performed using the two-microphone method.

For the extrapolation of the microphone signal recorded in the proximity of the engine, it is also necessary to know the isolating properties of the engine hood. This has been carried out using a set of microphones surrounding the hood surface over a semicircle for an estimation of the radiated sound power. The external signal due to the engine has been consequently propagated to the far-field in a similar way as it was done for the rolling noise, and both signals have been added at the position of the receiver.

A comparison between this prediction and the experimental data acquired at 7.5 m apart from the vehicle axis and at 1.2 m above the ground has been carried out, for pass-by velocities ranging from 40 to 90 km/h. The signal output from the rolling noise microphone has been filtered to account for aerodynamic and tyre noise directivity effects. A near-field filter has thus been selected and applied in the low frequency range as a function of the pass-by velocity. Besides the simplicity of the model, the comparison with the measurements is reasonably good, considering that most of the published results deal with a much more reduced frequency range of analysis. The accuracy in the overall levels predicted for the frequency range 20 Hz to 10 kHz stay within about 2 dB for all the pass-by velocities analysed. The proposed formulation constitutes then a consistent tool for traffic noise extrapolation.

Future work will be directed towards a validation of the results for a larger population of drivers, and will be extended to heavy and two-tyre vehicles, which are often the cause of high noise annoyance. We are also currently working in the improvement of the near-field filter for a better agreement of the overall levels between the propagation filter and the prediction.

Acknowledgment

We gratefully acknowledge the financial support of the Spanish Minister of Economy and Competitiveness, national Project TRA2011-26261-C04-01.

References

[1] Affenzeller J, Rust A. Road traffic noise- a topic for today and the future. In: Proc VDA Tech Congress 2005. Ingolstadt, Germany; 2005..
[2] Kragh J. News and needs in outdoor noise prediction. In: Proc Inter-noise 2001. The Hague, The Netherlands; 2001..
[3] Sandberg U. Noise emissions of road vehicles. Effect of regulations. Final Report 01–1, I-INCE WP-NERV; 2001..
[4] Bécot FX. Tyre noise impedance surfaces: efficient application of the Equivalent Source method. In: Ph.D. Thesis. France: Institute National des Sciences Appliquées de Lyon; 2003..
[5] Cesbron J, Anfosso-Lédée F, Duhamel D, Yin HP, LeHoué D. Experimental study of tyre/road contact forces in rolling conditions for noise prediction. J Sound Vib 2009;320(1–2):125–44.
[6] Anfosso-Lédée F. Acoustic monitoring of low noise road pavement. Noise Control Eng J 2009;57(2):50–62.
[7] Lui WK, Li KM. A theoretical study for the propagation of rolling noise over a porous road pavement. J Acoust Soc Am 2004;116(1):313–22.

[8] Beckenbauer T, Klein P, Hamet JF, Kropp W. Tyre/road noise prediction: a comparison between the SPERoN and HyRoNE models – Part 1. In: Proc Acoustics' 08. Paris, France; 2008..
[9] Beckenbauer T, Klein P, Hamet JF, Kropp W. Tyre/road noise prediction: a comparison between the SPERoN and HyRoNE models – Part 2. In: Proc Acoustics' 08. Paris, France; 2008..
[10] Sato T, Tano T, Bjorkman M, Rylander R. Road traffic noise annoyance in relation to average noise level, number of events and maximum noise level. J Sound Vib 1999;223(5):775–84.
[11] Ibarra D, Cobo P, Calvo JA, San Román JL. Relating the near field noise of passenger cars with the driving behavior. Noise Control Eng J 2012;60(2):171–83.
[12] Jonasson HL. Acoustic source modelling of road vehicles. Acust Acta Acust 2007;93:173–84.
[13] Stücklschwaiger W. Experimental pass-by noise source analysis. Report D.D10, Project Silence, CONTRACT N. 516288 European Commission; 2006..
[14] Sandberg U, Ejsmont JA. Tyre/road noise. Reference book. Kisa, Sweden: Informex; 2002.
[15] Anfosso-Lédée F. Modelling the local propagation effects of tyre-road noise: propagation filter between CPX and CPB measurements. In: Proc INTER-NOISE 2004. Prague, Czech Republic; 2004..
[16] Cho DS, Mun S. Determination of the sound power levels emitted by various vehicles using a novel testing method. Appl Acoust 2008;69(3):185–95.
[17] ISO 11819-1:1997. Acoustics-measurement of the influence of road surfaces on traffic noise – Part 1: statistical pass-by method. Geneva; 1997..
[18] ISO/CD 11819-2. Acoustics-measurement of the influence of road surfaces on traffic noise – Part 2: close-proximity method, draft document; 2000..
[19] ANSI S1.26, Calculation of the absorption of sound by the atmosphere. American National Standard, Acoustical Society of America; 1995 [R1999]..
[20] Berengier MC, Stinson MR, Daigle GA, Hamet JF. Porous road pavements: acoustical characterisation and propagation effect. J Acoust Soc Am 1997;101(1):155–62.
[21] Li KM, Waters-Fuller T, Attenborough K. Sound propagation from a point source over extended-reaction ground. J Acoust Soc Am 1998;104(2):679–85.
[22] Delany ME, Bazley EN. Acoustical properties of fibrous absorbent materials. Appl Acoust 1970;3(2):105–16.
[23] Bravo T, Ibarra D, Cobo P. Extrapolation of Maximum Noise Levels from near-field measurements to far-field positions. In: Proc INTER-NOISE 2012/ASME NCAD meeting. New York City, USA; 2012..
[24] ANSI S1.18. Template method for ground impedance. American National Standard, Acoustical Society of America; 1999..
[25] Kruse R, Mellert V. Effect and minimization of errors in situ ground impedance measurements. Appl Acoust 2008;69:884–90.
[26] Rasmussen KB. A note on the calculation of sound propagation over impedance jumps and screens. J Sound Vib 1982;84(4):598–602.
[27] Beranek LL, Vér IL. Noise and vibration control engineering. Principles and applications. New York: John Wiley & Sons; 1992.
[28] Pichaud Y, Anfosso-Lédée F. Caractérisation du bruit aérodynamique du Scénic LCPC Nantes. In: Rapport des mesures réalisées en soufflerie automobile anechoïque. Nantes, France: Laboratoire Central des Ponts et Chaussées; 2009.
[29] Anfosso-Lédée F. The development of a new tyre-road noise measurement device in France. In: Proc 5th Symp Pavement Surf Characteristics. Toronto, Canada; 2004..
[30] Mioduszewski P, Ejsmont J. Directivity of tyre/road noise emission of selected tyres and pavements. Noise Control Eng J 2009;57(2):129–38.